

CONCEPT ACTIVATION VECTORS: A UNIFYING VIEW AND ADVERSARIAL ATTACKS

Ekkehard Schnoor^{†‡}, Malik Tiomoko^{*}, Jawher Said[‡], Alex Jung[†], Wojciech Samek^{‡§}

[†] Department of Computer Science, Aalto University, Espoo, Finland

[‡] Department of Artificial Intelligence, Fraunhofer Heinrich Hertz Institute, Berlin, Germany

^{*} Huawei Noah's Ark Lab, Huawei Technologies, Paris, France

[§] Department of Electrical Engineering and Computer Science, Technical University Berlin, Germany

ABSTRACT

Concept Activation Vectors (CAVs) are a tool from explainable AI, offering a promising approach for understanding how human-understandable concepts are encoded in a model's latent spaces. They are computed from hidden-layer activations of inputs belonging either to a concept class or to non-concept examples. Adopting a probabilistic perspective, the distribution of the (non-)concept inputs induces a distribution over the CAV, making it a random vector in the latent space. This enables us to derive mean and covariance for different types of CAVs, leading to a unified theoretical view. This probabilistic perspective also reveals a potential vulnerability: CAVs can strongly depend on the rather arbitrary non-concept distribution, a factor largely overlooked in prior work. We illustrate this with a simple yet effective adversarial attack, underscoring the need for a more systematic study.

Index Terms— Concept Activation Vectors, Explainable AI (XAI), Deep Learning, Statistical Learning Theory

1. INTRODUCTION

Many XAI techniques generate attribution maps, highlighting important input regions for individual predictions. However, alone they provide limited insight, as often they do not specify what exactly the model has identified in those regions. Beyond mere feature-based explanations, *concept-based* explanations aim for explanations in terms of human-understandable concepts. Among them are CAVs [1], that perform linear probings to detect if human-understandable concepts are encoded in latent layers, and the related *Testing with Concept Activation Vectors (TCAV)*, that aims to quantify the contribution of a certain concept (e.g., *stripes*) to the prediction of a class (e.g. *zebras*). The original approach of [1] proposes classical linear classifiers like Support Vector

Machines (SVMs), Ridge Regression or the LASSO [2] to derive a CAV, which have been compared and applied for unlearning biases in [3]. Other methods for computing CAVs include *PatternCAV* [4], and the recently introduced *FastCAV* [5], both of which we will analyse more closely in this paper. While the aforementioned works consider applications in computer vision, CAVs were also applied successfully e.g. to analyse the acquisition of chess concepts during training by self-play in *AlphaZero* [6, 7]. Despite the successful applications of CAVs, a systematic understanding of their performance and robustness is still lacking. By construction, a CAV corresponds to the normal vector of a linear separator that distinguishes between (non-)concept activations.¹ This linear nature allows us to draw on the extensive body of work analyzing high-dimensional linear models with asymptotically sharp performance characterizations. We focus on the ridge regression [8, Chapter 2.3], and refer to similar works on SVMs [9], logistic regression [10], LASSO [11]. The classification accuracy of a CAV-based classifier can be interpreted as a measure for the degree to which a neural network has encoded a concept. It is of interest also in the context of Concept Bottleneck Models [12], which aim to increase the interpretability, typically at the price of a lower accuracy. In this paper, we propose a unifying probabilistic framework to investigate CAVs, enabling a more rigorous comparison of different CAV types by their distribution and classification performance. Our main contributions are as follows.

- We derive mean and covariance of *PatternCAV* [4] and *FastCAV* [5] in terms of the hidden-layer statistics in Proposition 1, allowing to predict their accuracies.
- We reveal the equivalence of seemingly different CAV methods the case of balanced classes² and large regularization parameter in the case of the ridge regression.
- We present an adversarial attack on the *TCAV* method.

This work was supported by the German Research Foundation (DFG) as research unit DeSBI [KI-FOR 5363] (459422098), by the Research Council of Finland (Decision #363624) as *A Mathematical Theory of Trustworthy Federated Learning (MATHFUL)*, by the Jane and Aatos Erkko Foundation (Decision #A835) as *A Mathematical Theory of Federated Learning (TRUST-FELT)*, and by Business Finland as *Forward-Looking AI Governance in Banking & Insurance (FLAIG)*.

¹Note that e.g. also for *PatternCAV* and *FastCAV*, an (optimal) separating hyperplane can be determined; therefore, we can interpret them as classifiers, even though they are not based on a classical linear classifier.

²This is not a strong restriction and typically the case in practice, as usually non-concept examples are cheap to obtain, making it easy to match the number of previously generated concept examples.

2. ASSUMPTIONS AND SETUP

Consider an L -layer neural network for classification, written as the concatenation $f_l \circ h_l$, where $f_l : \mathbb{R}^{d_0} \rightarrow \mathbb{R}^{d_l}$ is the mapping from the input (of size d_0) up to layer l (of size d_l); similarly, $h_l : \mathbb{R}^{d_l} \rightarrow \mathbb{R}^{d_L}$ is the mapping from the l th to the final L th layer. It is convenient to restrict ourselves to a specific class prediction, i.e., $h_{l,k} : \mathbb{R}^{d_l} \rightarrow \mathbb{R}$ is similar to h_l , but restricted to class k at the output. Assume we are given a set of examples collected by a user to illustrate some concept C of interest, as well as a set of *non-concept* (or “random”) examples (arbitrary input examples not containing the *concept* C , or noise). We may then train a linear classifier to separate their l th layer activations, and in this way obtain a CAV $\mathbf{v}_C^l \in \mathbb{R}^{d_l}$ that is orthogonal to the separating hyperplane (showing towards the concept region by convention). A high accuracy (of the CAV classifier) may be interpreted in the sense that the neural network has encoded the concept. While motivated by CAVs, we may often use a convenient compact notation considering a generic binary classification problem with a random training data matrix $\mathbf{X} = [\mathbf{x}_1, \dots, \mathbf{x}_n] \in \mathbb{R}^{d \times n}$ of n i.i.d. data points of feature size d and its associated label vector $\mathbf{y} = [y_1, \dots, y_n] \in \{-1, 1\}^d$ drawn from a mixture distribution of two classes with class-specific (conditional) mean $\boldsymbol{\mu}_\ell \in \mathbb{R}^d$ and covariance $\boldsymbol{\Sigma}_\ell \in \mathbb{R}^{d \times d}$ for $\ell = 1, 2$, and satisfying Assumption 1, for the n_ℓ vectors of class \mathcal{C}_ℓ , $\ell \in \{1, 2\}$; in particular, $n = n_1 + n_2$. Our goal is to predict the label y for a new test datum $\mathbf{x} \in \mathbb{R}^d$.

Assumption 1 (Data Concentration). *The random vector $\mathbf{x} \in \mathbb{R}^d$ is q -exponentially concentrated, i.e., for any 1-Lipschitz continuous (w.r.t. the ℓ_2 -norm) function $\varphi : \mathbb{R}^d \rightarrow \mathbb{R}$ it holds*

$$\mathbb{P}(|\varphi(\mathbf{x}_i) - \mathbb{E}[\varphi(\mathbf{x}_i)]| \geq t) \leq C e^{-(t/\sigma)^q} \quad \forall t > 0,$$

for some constants $q > 0$, $C > 0$, $\sigma > 0$ independent of d .

Random vectors satisfying Assumption 1 include isotropic Gaussian random vectors, the uniform distribution on the sphere, and notably any Lipschitz-continuous transformations thereof (e.g., features from GANs [13]). As (layers of) neural networks constitute Lipschitz-continuous functions, this framework is highly suitable in the context of CAVs.

We will use a result [8, Chapter 2.3] for the ridge regression which makes use of an “large n , large d ” assumption for its theoretical derivations, i.e., formally assuming that $n > d$ and, as $n_\ell, n, d \rightarrow \infty$, asymptotically $d/n \rightarrow c_0 \in (0, 1)$ and $n_\ell/n \rightarrow c_\ell > 0$ for $\ell = 1, 2$, with class probabilities c_1, c_2 ; often we will just consider the balanced case of $n_1 = n_2$ and therefore $c_1 = c_2 = 1/2$ with $c_1, c_2 \in (0, 1)$, $c_1 + c_2 = 1$. Still, the asymptotic prediction is often accurate in a finite but large-dimensional setting. Other results, notably our main result Proposition 1, hold in a non-asymptotic setting.

As CAVs perform a linear probing, we consider a linear classifier with weight vector $\mathbf{w} \in \mathbb{R}^d$ and bias $\eta \in \mathbb{R}$,

$$g(\mathbf{x}) = \frac{1}{\sqrt{n}} \mathbf{w}^\top \mathbf{x} \underset{c_1}{\overset{c_2}{\gtrless}} \eta. \quad (1)$$

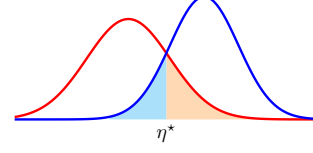


Fig. 1: Illust. of normal distributions of $g(\mathbf{x}) = \mathbf{x}^\top \mathbf{w}$ for $\mathbf{x} \in \mathcal{C}_1$ (red) and $\mathbf{x} \in \mathcal{C}_2$ (blue) with optimal decision threshold η^* at the intersection of the density function between the means.

Let us recall the following result, which enables us to predict in advance classification accuracies of linear classifiers, assuming class-specific normal distributions of the classification scores $g(\mathbf{x})$, which can be decomposed in terms of the data first and second-order statistics. We provide a generic statement; in the CAV context, the data corresponds to the hidden-layer activations of the *non-concept* (class \mathcal{C}_1 , label -1) vs. the *concept* (class \mathcal{C}_2 , label 1) examples. Note that this result has been used before, e.g. in [11]; still, to our best knowledge it has never been explored in the context of CAVs.

Theorem 1. *Let $\mathbf{w} \in \mathbb{R}^d$ be the (random) weight vector of the linear model g in (1), with mean $\bar{\mathbf{w}} = \mathbb{E}[\mathbf{w}]$ and covariance $\boldsymbol{\Sigma}_{\mathbf{w}} = \text{Cov}(\mathbf{w})$. Assume $g(\mathbf{x})$ to have class-specific normal distributions, i.e., $g(\mathbf{x}) \sim \mathcal{N}(m_\ell, \sigma_\ell^2)$ for (a test data point) of either class, i.e., $\mathbf{x} \in \mathcal{C}_\ell$ independent of \mathbf{w} , for $\ell = 1, 2$. Then, for $\mathbf{x} \in \mathcal{C}_\ell$ with mean $\boldsymbol{\mu}_\ell$ and covariance $\boldsymbol{\Sigma}_\ell$ it holds*

$$m_\ell = \frac{1}{\sqrt{n}} \mathbb{E}_{\mathbf{w}, \mathbf{x}} [\mathbf{w}^\top \mathbf{x}] = \frac{1}{\sqrt{n}} \bar{\mathbf{w}}^\top \bar{\mathbf{x}},$$

$$\sigma_\ell^2 = \frac{1}{n} \text{tr}(\boldsymbol{\Sigma}_{\mathbf{w}} \boldsymbol{\Sigma}_{\mathbf{x}}) + \frac{1}{n} \text{tr}(\boldsymbol{\Sigma}_{\mathbf{w}} \bar{\mathbf{x}} \bar{\mathbf{x}}^\top) + \frac{1}{n} \text{tr}(\boldsymbol{\Sigma}_{\mathbf{x}} \bar{\mathbf{w}} \bar{\mathbf{w}}^\top).$$

Consequently, the (optimal) classification accuracy of (1) is given by $1 - \varepsilon$, where the probability of misclassification ε is

$$\begin{aligned} \varepsilon &= c_1 \cdot \mathbb{P}(\mathbf{x} \rightarrow \mathcal{C}_2 | \mathbf{x} \in \mathcal{C}_1) + c_2 \cdot \mathbb{P}(\mathbf{x} \rightarrow \mathcal{C}_1 | \mathbf{x} \in \mathcal{C}_2) \\ &= c_1 \cdot \mathbb{P}(X > \eta | X \sim \mathcal{N}(m_1, \sigma_1^2)) + \\ &\quad c_2 \cdot \mathbb{P}(Y < \eta | Y \sim \mathcal{N}(m_2, \sigma_2^2)), \end{aligned} \quad (2)$$

where $\eta \in \mathbb{R}$ denotes the (optimal) decision threshold in (1).

Proof. The formulas for m_ℓ and σ_ℓ^2 follow from a straightforward computation of the mean and variance, by the independence of \mathbf{w} and \mathbf{x} (and even hold without the assumption of Gaussianity). The formula for ε is due to the classification rule (1) and the assumption of $g(\mathbf{x})$ to be Gaussian. \square

The two summands adding up to ε in (2) correspond to the areas of respective color in Fig. 1. Notably, the classification accuracy only depends on the few scalars $m_1, m_2, \sigma_1^2, \sigma_2^2$, from which it can be computed by numerical integration of the normal distribution’s CDF. To obtain those scalars, we need to estimate both the data as well as the model’s means and covariances. While in practice both are simply estimated

empirically from the training data, deriving the induced distribution over \mathbf{w} is challenging (see Sec. 3). Finally, we remark that the assumption of normal distributions of $g(\mathbf{x})$ in (1) is highly realistic under Assumption 1 and has been often observed in practice; see [14, Theorem 3.2] and [15, 16] for a version of the central limit theorem for concentrated random vectors. Next, let us recall a few different methods to compute CAVs, preparing for our main results in the next section, which includes an application of Theorem 1 for the different ways to compute the CAV, corresponding to the weight vector \mathbf{w} . One way to obtain the CAV \mathbf{w} is by the *ridge regression*

$$\mathbf{w}_{\text{ridge}} = \arg \min_{\mathbf{w} \in \mathbb{R}^d} \left\| \mathbf{y} - \frac{\mathbf{X}^\top}{\sqrt{n}} \mathbf{w} \right\|_2^2 + \lambda \|\mathbf{w}\|_2^2. \quad (3)$$

We solve (3) by [8, Chapter 2.3] - see also [17] -, iteratively computing m_ℓ, σ_ℓ^2 with $\mathbf{w} = \mathbf{w}_{\text{ridge}}$, for $\ell = 1, 2$. As an alternative method to compute CAVs, the *PatternCAV* [4] is

$$\mathbf{w}_{\text{pat}} = \arg \min_{\mathbf{w} \in \mathbb{R}^d} \left\| \mathbf{X}^\top - \mathbf{y} \mathbf{w}^\top \right\|_2^2 \quad (4)$$

$$= \frac{1}{n_2} \sum_{i=1}^{n_2} \mathbf{x}_i^{(2)} - \frac{1}{n_1} \sum_{i=1}^{n_1} \mathbf{x}_i^{(1)}, \quad (5)$$

showing in the direction of $\boldsymbol{\mu}_2$, towards the concept region. For the recently proposed *FastCAV* [5] we begin by computing the joint empirical mean of both classes, denoted by $\hat{\boldsymbol{\mu}}_{1,2}$,

$$\hat{\boldsymbol{\mu}}_{1,2} = \frac{1}{n_1 + n_2} \sum_{\ell=1}^2 \sum_{i=1}^{n_i} \mathbf{x}_i^{(\ell)} \in \mathbb{R}^d. \quad (6)$$

The *FastCAV* is the vector pointing from the global mean $\hat{\boldsymbol{\mu}}_{1,2}$ towards the mean of the concept class, *i.e.*, \mathcal{C}_2 . Formally, it is

$$\mathbf{w}_{\text{fast}} = \frac{1}{n_2} \sum_{i=1}^{n_2} \left(\mathbf{x}_i^{(2)} - \hat{\boldsymbol{\mu}}_{1,2} \right) = \frac{1}{n_2} \sum_{i=1}^{n_2} \mathbf{x}_i^{(2)} - \hat{\boldsymbol{\mu}}_{1,2}. \quad (7)$$

3. MAIN RESULTS AND EXPERIMENTS

We present our theoretical main results, together with experiments³ on simple synthetic data like Gaussian Mixture Models (GMMs) for binary classification, as well as the *ResNet-18* model applied to the *CIFAR-10* dataset, and a simple neural network with three hidden layers for times series classification trained by ourselves, with the time series input given by

$$y(t) = A \cdot \sin(2\pi \cdot f \cdot t) + T \cdot t + \varepsilon, \quad t = 0, \dots, T, \quad (8)$$

with amplitude A , frequency f , trend T and noise ε . The classes are characterized by (a combination of) high or low values for A , f and T (presence or absence of the concepts).

³We provide code to reproduce our experiments in this Github repository: github.com/jawhar00/cav-unifying-view-adversarial

3.1. Classification Accuracies of CAVs

We adopt a probabilistic standpoint, interpreting CAVs as random vectors in latent space whose distribution is induced by the non-linear transformations of the (non-)concept input distributions. This provides new insights into recently suggested techniques for computing CAVs. While relying on [8, Chapter 2.3] for ridge regression (3), our main theoretical result derives the distributions of *PatternCAV* (5) and *FastCAV* (7), revealing their performances and surprisingly close relation.

Proposition 1. [Distribution of \mathbf{w}_{fast} and \mathbf{w}_{pat}] Mean and covariance of \mathbf{w}_{fast} and \mathbf{w}_{pat} can be compactly expressed in terms of the data distribution as follows. Assuming class-specific means $\boldsymbol{\mu}_\ell$ and covariances $\boldsymbol{\Sigma}_\ell$ for $\ell = 1, 2$, it holds

$$\mathbb{E}[\mathbf{w}_{\text{pat}}] = \bar{\mathbf{w}}_{\text{pat}} = \boldsymbol{\mu}_2 - \boldsymbol{\mu}_1 \in \mathbb{R}^d, \quad (9)$$

$$\text{Cov}(\mathbf{w}_{\text{pat}}) = \boldsymbol{\Sigma}_{\mathbf{w}_{\text{pat}}} = \frac{1}{n_1} \boldsymbol{\Sigma}_1 + \frac{1}{n_2} \boldsymbol{\Sigma}_2 \in \mathbb{R}^{d \times d}, \quad (10)$$

For $n_1 = n_2$, \mathbf{w}_{fast} is a scaled version⁴ of \mathbf{w}_{pat} as $\mathbf{w}_{\text{fast}} = \frac{1}{2} \mathbf{w}_{\text{pat}}$. Consequently, the mean and covariance of $\bar{\mathbf{w}}_{\text{fast}}$ are

$$\mathbb{E}[\bar{\mathbf{w}}_{\text{fast}}] = \bar{\mathbf{w}}_{\text{fast}} = \frac{\boldsymbol{\mu}_2 - \boldsymbol{\mu}_1}{2} \in \mathbb{R}^d, \quad (11)$$

$$\text{Cov}(\bar{\mathbf{w}}_{\text{fast}}) = \boldsymbol{\Sigma}_{\bar{\mathbf{w}}_{\text{fast}}} = \frac{1}{4n_1} \boldsymbol{\Sigma}_1 + \frac{1}{4n_2} \boldsymbol{\Sigma}_2 \in \mathbb{R}^{d \times d}. \quad (12)$$

Proof. The case of the mean (9) is obvious, and (10) concerning the covariance follows from a straightforward computation starting from (5). Next, we then obtain the scaling,

$$\mathbf{w}_{\text{fast}} = \frac{1}{n_2} \sum_{i=1}^{n_2} \mathbf{x}_i^{(2)} - \frac{1}{2n_1} \sum_{i=1}^{n_1} \mathbf{x}_i^{(1)} - \frac{1}{2n_2} \sum_{i=1}^{n_2} \mathbf{x}_i^{(2)} = \frac{1}{2} \mathbf{w}_{\text{pat}},$$

only by (5) and (7), immediately yielding (11) and (12). \square

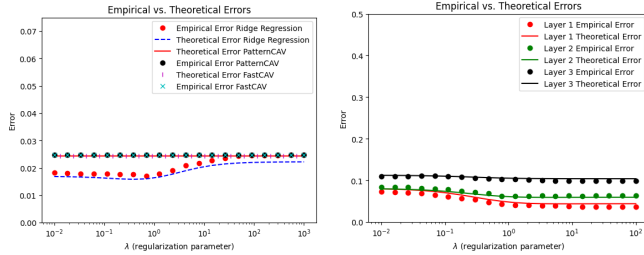
Remark 1 (Relationship between \mathbf{w}_{fast} , \mathbf{w}_{pat} and $\mathbf{w}_{\text{ridge}}$). It turns out that \mathbf{w}_{pat} , and by $\mathbf{w}_{\text{fast}} = \frac{1}{2} \mathbf{w}_{\text{pat}}$, also \mathbf{w}_{fast} , are closely related to the case of ridge regression, since for sufficiently large $\lambda = O(\sqrt{n})$, by simply inserting $\lambda = \sqrt{n}$,

$$\begin{aligned} \mathbf{w}_{\text{ridge}} &= \left(\frac{1}{n} \mathbf{X} \mathbf{X}^\top + \lambda \mathbf{I}_p \right)^{-1} \frac{\mathbf{X}}{\sqrt{n}} \mathbf{y} \approx \frac{1}{\lambda} \mathbf{I}_p \frac{\mathbf{X}}{\sqrt{n}} \mathbf{y} \quad (13) \\ &= \frac{1}{n} \sum_{i=1}^n y_i \mathbf{x}_i = \frac{1}{n} \left(\sum_{i=1}^{n_2} \mathbf{x}_i^{(2)} - \sum_{i=1}^{n_1} \mathbf{x}_i^{(1)} \right) = \frac{1}{2} \mathbf{w}_{\text{pat}}. \end{aligned}$$

Even though the hyperplane is the primary object of interest in *TCAV*, Proposition 1 further allows us to derive the associated classification accuracy, which, while not essential for the computation of *TCAV* itself, provides valuable theoretical insight into the reliability of concept encoding. As the error ε from (2) remains unchanged when scaling \mathbf{w} (assuming $g(\mathbf{x})$ is normally distributed), \mathbf{w}_{pat} and \mathbf{w}_{fast} turn out to

⁴More generally, in the unbalanced case, $\mathbf{w}_{\text{fast}} = n_1 / (n_1 + n_2) \mathbf{w}_{\text{pat}}$.

have exactly the same accuracies as classifiers, and a performance similar to ridge regression for sufficiently large λ . This is confirmed by the experiments on synthetic data in Fig. 2a. Fig. 2b is similar to Fig. 2a, with ridge regression applied to the activations of the (non-)concept examples in the time series model, comparing errors for different layers. Fig. 3 is similar to the illustration in Fig. 1, for different layers of the *ResNet-18* model [18] and *CIFAR-10* dataset [19], comparing theoretical prediction and empirical findings on the test set.



(a) Errors of *ridge regression* (plotted over λ), *FastCAV* and *freq.* vs. non-concept noise $\mathbf{x} \sim \text{PatternCAV}$ (constant, repeated $\mathcal{N}(\mathbf{0}, \mathbf{I})$ (at input); ε at their l - for λ) for synthetic data (GMM). (b) Time series (8): concept *high* (plotted over λ), *FastCAV* and *freq.* vs. non-concept noise $\mathbf{x} \sim \text{PatternCAV}$ (constant, repeated $\mathcal{N}(\mathbf{0}, \mathbf{I})$ (at input); ε at their l - for λ) for synthetic data (GMM). tent layers activations (colors).

Fig. 2: Accurate theoretical prediction of the classification error ε from (2) as a function of λ (*ridge regression*); different colors refer to different methods 2a or different layers 2b.

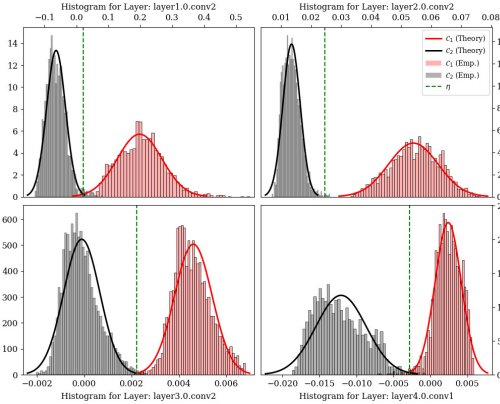


Fig. 3: Close match between test-set histograms and the Gaussian predictions of the CAV projection for the concept *blue* vs. noise $\mathbf{x} \sim \mathcal{N}(\mathbf{0}, \mathbf{I})$; ridge-regression (fixed λ), for different layers (*ResNet-18* model for the *CIFAR-10* dataset).

3.2. TCAV Scores and Adversarial Attacks

To quantify the contribution of a concept C to the prediction of class C_k for an input example $\mathbf{x} \in \mathbb{R}^{d_0}$ based on a CAV \mathbf{v}_C^l at layer l , a sensitivity score $S_{C,k,l}(\mathbf{x})$ has been proposed [1],

$$S_{C,k,l}(\mathbf{x}) = \lim_{h \rightarrow 0} \frac{h_{l,k}(f^l(\mathbf{x}) + h \cdot \mathbf{v}_C^l) - h_{l,k}(f^l(\mathbf{x}))}{h} = \langle \nabla h_{l,k}(f^l(\mathbf{x})), \mathbf{v}_C^l \rangle, \quad (14)$$

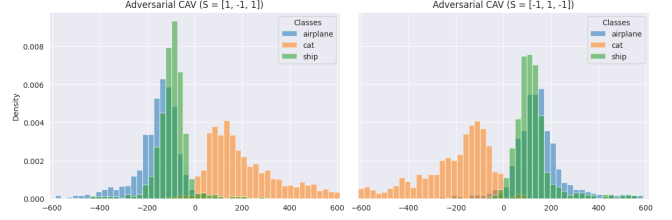


Fig. 4: Histograms of $S_{C,k,l}(\mathbf{x})$ from (14) with \mathbf{x} from 3 classes (colors) at layer **layer3.0.conv2** of the *ResNet-18* model for the *CIFAR-10* dataset; using two different choices of $S = (s_1, s_2, s_3)$ to manipulate the CAV, and thus the histograms of the scores $S_{C,k,l}(\mathbf{x})$, as well as $\text{TCAV}_{Q_C,k,l}$.

i.e., the directional derivative of $h_{l,k}$ in direction of \mathbf{v}_C^l , equivalent to (14) under sufficient smoothness assumptions. To quantify the overall contribution of concept C to class C_k , [1] introduced a score $\text{TCAV}_{Q_C,k,l} \in [0, 1]$, measuring the percentage of $S_{C,k,l}(\mathbf{x})$ being positive for $\mathbf{x} \in C_k$, or formally,

$$\text{TCAV}_{Q_C,k,l} = \frac{|\{\mathbf{x} \in \mathcal{X}_k : S_{C,k,l}(\mathbf{x}) > 0\}|}{|\mathcal{X}_k|} \in [0, 1].$$

Note that $S_{C,k,l}(\mathbf{x})$ and $\text{TCAV}_{Q_C,k,l}$ may strongly depend on the specific choice of \mathbf{v}_C^l , which in turn depends on the method to compute it, and on the rather arbitrary choice of the non-concept data distribution. In [1], randomized CAVs were computed repetitively. We aim to initiate a more systematic investigation, starting with the worst-case scenario by proposing an adversarial attack. For a K -class classification problem with class-wise data matrices $\mathbf{X}^{(k)}$, corresponding to the hidden-layer activations in the CAV context, consider a sign $s_k = \pm 1$. This may or may not be the “correct” sign for C_k , but the sign we want to *avoid* in an adversarial setting, where we would like to “push the sensitivity scores of $\mathbf{X}^{(k)}$ away from s_k ” (driving $\text{TCAV}_{Q_C,k,l}$ either closer to 0 or 1), *i.e.*, we would like to enforce that $s_k \cdot \mathbf{X}^{(k)} \mathbf{w} < 0$ “for many entries”. Precisely, we propose to minimize $\sum_{k=1}^K \mathbb{1}_{\{s_k \cdot \mathbf{X}^{(k)} \mathbf{w} > 0\}}$, where $\mathbb{1}_{\{z > 0\}} := \sum_{i=1}^p \mathbb{1}_{\{z_i > 0\}}$ counts the number of positive entries of $\mathbf{z} \in \mathbb{R}^p$; for the implementation, we use a smooth approximation by the sigmoid function $\sigma(x) = 1/(1 + e^{-x})$, as illustrated in Fig. 4.

4. CONCLUSION AND OUTLOOK

We described the distributions of *PatternCAV* and *FastCAV*, enabling to predict their classification accuracy, revealing their close connection to each other and to ridge regression. We proposed an adversarial attack at the latent space as a worst-case scenario that manipulates explanations, leaving a general investigation of CAV’s robustness for future work.

5. REFERENCES

- [1] Been Kim, Martin Wattenberg, Justin Gilmer, Carrie Cai, James Wexler, Fernanda Viegas, et al., “Interpretability beyond feature attribution: Quantitative testing with concept activation vectors (tcav),” in *International conference on machine learning*. PMLR, 2018, pp. 2668–2677.
- [2] Robert Tibshirani, “Regression selection and shrinkage via the lasso,” *Journal of the Royal Statistical Society Series B*, vol. 58, no. 1, pp. 267–288, 1996.
- [3] Maximilian Dreyer, Frederik Pahde, Christopher J Anders, Wojciech Samek, and Sebastian Lapuschkin, “From hope to safety: Unlearning biases of deep models via gradient penalization in latent space,” in *Proceedings of the AAAI Conference on Artificial Intelligence*, 2024, vol. 38, pp. 21046–21054.
- [4] Frederik Pahde, Maximilian Dreyer, Leander Weber, Moritz Weckbecker, Christopher J Anders, Thomas Wiegand, Wojciech Samek, and Sebastian Lapuschkin, “Navigating neural space: Revisiting concept activation vectors to overcome directional divergence,” *arXiv preprint arXiv:2202.03482*, 2022.
- [5] Laines Schmalwasser, Niklas Penzel, Joachim Denzler, and Julia Niebling, “Fastcav: Efficient computation of concept activation vectors for explaining deep neural networks,” in *Proceedings of the 42nd International Conference on Machine Learning (ICML)*, 2025.
- [6] Thomas McGrath, Andrei Kaphishnikov, Nenad Tomašev, Adam Pearce, Martin Wattenberg, Demis Hassabis, Been Kim, Ulrich Paquet, and Vladimir Kramnik, “Acquisition of chess knowledge in alphazero,” *Proceedings of the National Academy of Sciences*, vol. 119, no. 47, pp. e2206625119, 2022.
- [7] Lisa Schut, Nenad Tomasev, Tom McGrath, Demis Hassabis, Ulrich Paquet, and Been Kim, “Bridging the human-ai knowledge gap: Concept discovery and transfer in alphazero,” *CoRR*, 2023.
- [8] Malik Tiomoko, *Advanced Random Matrix Methods for Machine Learning*, Ph.D. thesis, Université Paris-Saclay, 2021.
- [9] Zhenyu Liao and Romain Couillet, “A large dimensional analysis of least squares support vector machines,” *IEEE Transactions on Signal Processing*, vol. 67, no. 4, pp. 1065–1074, 2019.
- [10] Xiaoyi Mai, Zhenyu Liao, and Romain Couillet, “A large scale analysis of logistic regression: Asymptotic performance and new insights,” in *ICASSP 2019-2019 IEEE International Conference on Acoustics, Speech and Signal Processing (ICASSP)*. IEEE, 2019, pp. 3357–3361.
- [11] Malik Tiomoko, Ekkehard Schnoor, Mohamed El Amine Seddik, Igor Colin, and Aladin Virmaux, “Deciphering lasso-based classification through a large dimensional analysis of the iterative soft-thresholding algorithm,” in *International Conference on Machine Learning*. PMLR, 2022, pp. 21449–21477.
- [12] Pang Wei Koh, Thao Nguyen, Yew Siang Tang, Stephen Mussmann, Emma Pierson, Been Kim, and Percy Liang, “Concept bottleneck models,” in *Proceedings of the 37th International Conference on Machine Learning*, Hal Daumé III and Aarti Singh, Eds. 13–18 Jul 2020, vol. 119 of *Proceedings of Machine Learning Research*, pp. 5338–5348, PMLR.
- [13] Mohamed El Amine Seddik, Cosme Louart, Mohamed Tamaazousti, and Romain Couillet, “Random matrix theory proves that deep learning representations of gan-data behave as gaussian mixtures,” in *International Conference on Machine Learning*. PMLR, 2020, pp. 8573–8582.
- [14] Mohamed El Amine Seddik, Cosme Louart, Romain Couillet, and Mohamed Tamaazousti, “The unexpected deterministic and universal behavior of large softmax classifiers,” in *International Conference on Artificial Intelligence and Statistics*. PMLR, 2021, pp. 1045–1053.
- [15] Bo’az Klartag, “A central limit theorem for convex sets,” *Inventiones mathematicae*, vol. 168, no. 1, pp. 91–131, 2007.
- [16] Bruno Fleury, Olivier Guédon, and Grigoris Paouris, “A stability result for mean width of l_p -centroid bodies,” *Advances in Mathematics*, vol. 214, no. 2, pp. 865–877, 2007.
- [17] Hamza Cherkaoui, Malik Tiomoko, Mohamed El Amine Seddik, Cosme Louart, Ekkehard Schnoor, and Balazs Kegl, “High-dimensional analysis of bootstrap ensemble classifiers,” *arXiv preprint arXiv:2505.14587*, 2025.
- [18] Kaiming He, Xiangyu Zhang, Shaoqing Ren, and Jian Sun, “Deep residual learning for image recognition,” in *Proceedings of the IEEE Conference on Computer Vision and Pattern Recognition (CVPR)*, 2016, pp. 770–778.
- [19] Alex Krizhevsky, Geoffrey Hinton, et al., “Learning multiple layers of features from tiny images,” 2009.